The Effect of Glucose on Erythrocyte Morphology and Optical Scattering of Human Whole Blood

Jared Roth

A senior thesis submitted to the faculty of
Brigham Young University
in partial fulfillment of the requirements for the degree of

Bachelor of Science

Dr. Richard Vanfleet and Dr. Robert Davis, Advisors

Department of Physics and Astronomy

Brigham Young University

ABSTRACT

The Effect of Glucose on Erythrocyte Morphology and
Optical Scattering of Human Whole Blood

Jared Roth
Department of Physics and Astronomy, BYU
Bachelor of Science

The need for accurate blood glucose monitoring cannot be understated. Current techniques to determine glucose concentration are invasive and uncomfortable. Previous work [1] has shown a response in the optical properties (specifically the scattering coefficient) of fresh, whole, human blood following an increase in glucose concentration. Clarifying the relationship between glucose concentration and blood optical properties may lead to developments in noninvasive glucose monitoring.

In the present work, the effects of elevated glucose concentrations on the morphology of fresh, human erythrocytes were measured in-vitro. To determine potential mechanisms for the change in the scattering coefficient, optical microscopy was employed to quantify the change in erythrocyte geometry. A 15% change in average cell thickness was observed following a glucose increase of +500 mg/dL. This corresponded to an increase of +0.059 μm for each glucose concentration step of +100 mg/dL. Significant portions of this work are reported elsewhere [2].

Keywords: Erythrocyte, Glucose, Light Scattering, Optical Microscopy, Morphology

ACKNOWLEDGMENTS

I want to acknowledge the financial and technical support of Octavian solutions. This project would not have been possible without their funding and advice.

I would like to thank my advisors, Dr. Davis and Dr. Vanfleet for pushing me to think deeply about my research questions and to embrace the process of finding the right question. I also want to thank my lab-mates, especially James, for training me and showing me how to really get my hands on the experiment.

I especially want to thank Mom, Dad, and Kyle who helped me become a scientist in the first place. Thank you for believing in me from day one. Thank you for encouraging me through the highs and particularly through the lows.

Most of all, I want to thank Ruth. You've helped me so much through classes, research, and life in general. Thank you for letting me talk through my experiments with you and thank you for being a nerd with me. Thank you for always helping me become a better person.

Contents

List of Figures

List of Tables

Chapter 1

Introduction

Significant portions of this work are reported in an SPIE Photonics West Conference manuscript [2]. One may also find a more detailed description of the experimentation on optical properties in the work of Harkness et al. [1]

1.1 Diabetes

As of April 2024, 38.4 million Americans have diabetes, which represents 11.8% of the US population. An additional 97.6 million (38%) adults have prediabetes [3]. Diabetes is currently the 8th leading cause of death in the United States and the world. It can have many detrimental effects on the body including nerve damage, kidney damage, blindness, and cardiovascular disease. Diabetes is the inability of the body to self-regulate glucose concentration. This may occur from the body not producing enough insulin (Type I diabetes) or from muscle and fat cells losing sensitivity to insulin (Type II diabetes). Patients with diabetes must closely regulate their blood sugar (glucose) levels.

Several glucose monitors have been developed to allow close tracking of glucose concentration. However, these monitors require direct contact with blood or interstitial fluid. Finger pricking

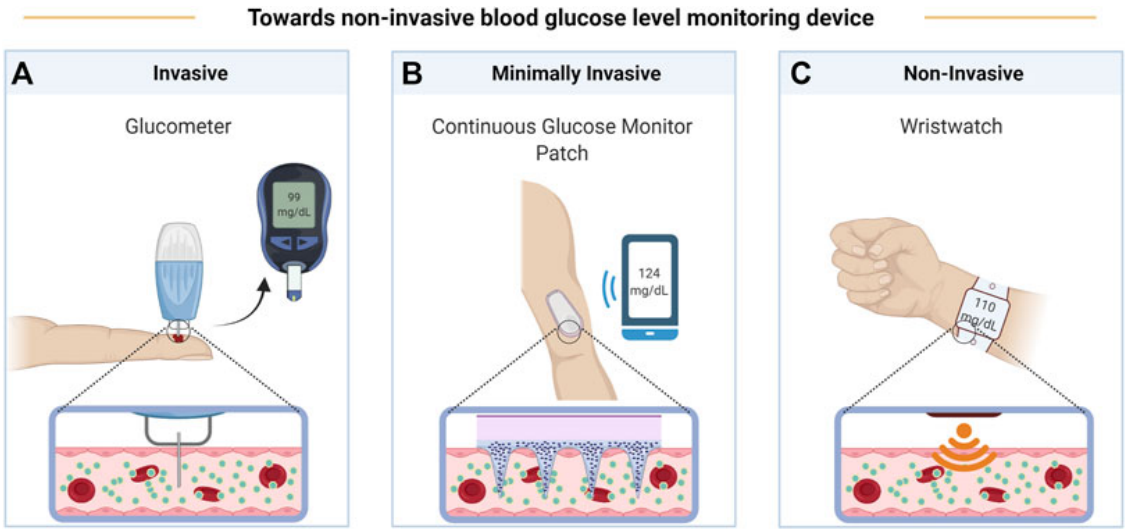

Figure 1.1 Various glucose monitoring techniques. A) Finger pricking used with a glucometer. B) Continuous glucose monitoring patch. C) Theoretical noninvasive glucose monitoring wristwatch. Image credit: Todaro et al. [4]

devices and continuous patch monitors both break the skin and can be painful, inconvenient, and may lead to infection. Figs. 1.1A and 1.1B (taken from Todaro et al. [4]) shows several glucose monitoring techniques. While some glucose monitoring devices have been proposed that do not break the skin, no noninvasive glucose monitoring devices have been approved by the FDA [5].

1.2 Noninvasive Glucose Monitoring

The value of continuous noninvasive glucose monitoring is immense. Real-time and continuous feedback would enable more accurate tracking of glucose concentrations and thus allow the patient to take necessary steps quickly if the concentration leaves the desired range. The noninvasive aspect would render glucose tracking significantly more comfortable and would eliminate the risk of infection. See Fig. 1.1C.

Numerous noninvasive methods are currently under investigation. These methods can be grouped into five main categories (as proposed by Pullano et al. [6]): Raman spectroscopy, optical coherence

tomography, photoacoustic spectroscopy, fluorescence, and near infrared (NIR) spectroscopy. Several NIR studies [1, 7] have shown that glucose concentration affects the scattering properties of whole blood. Thus, infrared measurement of the scattering properties of blood could potentially be used to indirectly measure glucose concentration in the blood.

1.3 Optics

Like all materials, blood has quantifiable optical properties (including refractive index, coefficient of absorption, reduced scattering coefficient, and anisotropy factor). Our lab's objective is to relate these optical properties to glucose concentration.

The Beer-Lambert law,

$$I = I_0 e^{-(\mu_a + \mu_s)x}, \tag{1.1}$$

describes the decrease of intensity of light, I, as it propagates through a medium. The coefficient of absorption, μ_a, and the coefficient of scattering, μ_s, are the principal components of light attenuation. x is the penetration depth and I_0 is the initial intensity of the light. While the absorption of blood is mostly dominated by the water absorption spectrum, the scattering is likely due to the mismatch between the indices of refraction of the plasma and the scattering bodies (mostly erythrocytes).

It should be noted that classical ray optics will not dictate the propagation of light through blood. Likewise, Rayleigh scattering is a poor model for this system because the scattering bodies are not significantly smaller than the wavelength of light, as required by the Rayleigh model. For scattering body dimensions and wavelengths that are nearly equal, Mie scattering gives a better approximation. Understanding of a correct scattering model is necessary as it will dictate which optical properties are important. For example, the scattering coefficient, μ_s, is a principal optical parameter for blood whereas refractive index of whole blood is likely less informative. Additionally, choosing the proper scattering model will shed light on future optical modeling research (see Section 4.2).

Our recent work, reported in Harkness et al. [1], has shown that fresh, whole, human blood *in vitro* will undergo a change in the scattering and absorption coefficients following an increase in glucose concentration. This has been shown in the wavelength range from 1100 nm to 1800 nm.

1.4 Erythrocyte Morphology

In order to discuss cell morphology and solution concentrations, there are several terms than need to be defined. It is important to distinguish between these terms because, while they are related, they each have specific meanings and are often mistaken for each other.

Molarity is defined as the number of moles of a particular analyte divided by the volume of the solution. It has units of $\frac{mols}{L}$, which may be referred to as a "molar". Molality is defined as the number of moles of a particular analyte dissolved in a certain mass of solvent. It has units of $\frac{mols}{kg}$ and can be referred to as a "molal". Even though these two quantities are related, they may differ under certain circumstances. For example, molality is temperature independent whereas solution molarity may change with temperature as the solvent expands or contracts. Take, for example, a 0.2 molar aqueous solution of HCl at $3.984°C$. At this specific temperature, $1\ L\ H_2O = 1\ kg\ H_2O$. Thus, the solution would also be a 0.2 molal solution. As the solution increases in temperature, the solvent will maintain a constant mass but will increase in volume. This will render the solution a less-than-0.2 molar solution, but it will remain a 0.2 molal solution regardless of temperature.

Osmolality is defined as the number of dissolved particles per mass of solvent. In the case of aqueous glucose, osmolality equals molality since glucose molecules don't dissociate in water. A comparison between the osmolality of two solutions is frequently needed. If solution A is being added to solution B, the relative osmolalities can be compared. If solution A has a lower osmolality than solution B, then it is considered "hypoosmotic". If it has a greater osmolality, it is considered "hyperosmotic". If the two solutions have the same osmolality, they are considered "isosmotic".

Tonicity of a solution is defined based purely on the qualitative effect the solution has when added to biological cells. If a solution causes the cells to swell, the solution is considered "hypotonic". If the added solution causes the cells to shrivel and/or shrink, the solution is "hypertonic". If the solution has no effect on the cells' morphology, the solution is considered "isotonic". Most of the time, isosmotic solutions are also isotonic. Likewise, hyposmotic and hypotonic as well as hyperosmotic and hypertonic are nearly always synonymous. Further details regarding the distinction between these values and their effect in the blood of large animals can be found in Chapter 5 of *Veterinary Medicine* by Constable et al. [8]

Because of these effects, this study was conducted using isosmotic aqueous glucose additions which had an osmolality within the physiological range (275 to 295 mOsmol/kg). This ensured that any change in erythrocyte morphology was due to the increase in glucose concentration, and not the tonicity of the addition.

It should be noted that there are many differences between human blood *in vivo* and *in vitro*. These various differences may affect the optical properties of the blood as well as the morphology of the erythrocytes. However, this study revealed that fresh human erythrocytes drawn from healthy donors (see Chapter 2 for methods) have similar cell dimensions to the cells *in vivo* (see the introductory paragraph of Chapter 4). This fact suggests that fresh, whole, human blood can be used as a good approximation for blood *in vivo* when specifically considering erythrocyte morphology.

Among the differences between blood *in vitro* and *in vivo* is the fact that blood in a test tube or on a coverslip is stagnant rather than dynamic. While there are a number of differences between stagnant and dynamic (flowing) blood, the morphology of erythrocytes is generally consistent [9], again supporting the comparison of our work to cells *in vivo*. Stagnant blood cells quickly aggregate and create Rouleaux formations, which are stacks of erythrocytes. *In vivo*, the flow of blood inhibits significant quantities of Rouleaux formations. The average number of cells in a Rouleaux formation

(as well as the number of formations) is inversely proportional to the flow rate of blood [10]. Rouleaux formations provided a valuable tool to measure average cell thickness (see Section 2.2).

1.5 A Mechanistic Explanation

The mechanism behind the optical scattering changes following glucose addition is not completely clear. However, morphological changes in erythrocytes have been shown to affect scattering. Cells *in vivo* are known to frequently undergo morphological changes. For example, nearly all cells have thermal undulations, which are small vibrations of the cell membrane caused by the nonzero translational energy of molecules. An example unique to erythrocytes is the incredible deformability of the cells as they pass through the narrow capillaries of the body.

"Mauer et al. [11] have demonstrated numerically that even the thermal undulations of erythrocytes should be detectable using dynamic light scattering. These undulations are typically on the order of 10-400 nm [12]. Borovoi et al. [13] employed a straight-ray approximation with a plane wave receiving a complex phase shift as it passed through the cell. They found cell dimensions to have a measurable effect on the scattered light. Streekstra et al. [14] employed an ektacytometer, which measured deformability and ellipticity of the erythrocytes. They demonstrated that cell morphology affects scattering properties. Sloot, Figdor, and Hoekstra used a modified Rayleigh-Gans-Debye scattering model. They showed both numerically [15] and experimentally [16] that forward scattering from osmotically shocked lymphocytes was dependent on their morphology. In short, these studies have shown that cell shape and dimension will affect the optical scattering of blood." (Quotation from Roth et al. [2])

The goal of this research has been to quantify the effect of glucose concentration on erythrocyte morphology *in vitro*. This will inform future studies seeking to relate glucose concentration in whole, human blood to optical properties.

Chapter 2

Methods

The purpose of this experiment was to quantify the effect of elevated glucose concentration on erythrocyte morphology. This chapter describes the procedure for how fresh, whole, human blood received a glucose addition that increased glucose concentration while maintaining physiological osmolality. Erythrocyte dimensions were then analyzed using optical microscopy.

2.1 Blood Collection and Glucose Addition

Two healthy adults provided whole blood donations in accordance with BYU Institutional Review Board #X-2021-135. One blood sample was collected on 11/5/25 and the other was on 12/9/25. The blood was drawn into BD Vacutainer EDTA Blood Collection Tubes. All experimentation was conducted within 6 hours of the blood draw (this is what is meant when the blood is referred to as "fresh").

An aqueous glucose solution of concentration 5400 mg/dL (which is near physiological osmolality of 275 to 295 mOsmol/L) was prepared. The starting glucose concentration of the donated blood was measured using a Tula Genie Glucometer. For the 11/5 experiment, the blood was divided into 3 test tubes, each containing 1 mL whole blood. The isosmotic glucose solution was added to

each vial in a quantity that changed the glucose concentration by a known amount (+0, +1000, or +2000 mg/dL). Immediately following the glucose additions, the vials were inverted slowly to mix the blood. The 12/9 experiment was identical except that 5 test tubes were used (each with 1 mL whole blood). Again, glucose was added to change the concentration by known amounts (+0, +500, +1000, +1500 or +2000 mg/dL).

2.2 Erythrocyte Morphology Experimentation

Due to plasma separation after the blood draw, the vial was gently mixed by inverting several times. A pipette was then used to draw approximately 5 μL whole blood and place it on a microscope coverslip. Then, a second coverslip was placed on top of the blood, causing a very thin, nearly uniform layer of blood between the two coverslips.

The blood samples were examined using a Keyence VHX Optical microscope equipped with a 4K complimentary metal-oxide semiconductor (CMOS) image sensor and a numerical aperture (NA) of 0.9. The full-coaxial setting was selected for illumination (see Fig. 2.1). The blood between coverslips was placed on the microscope observation stage. 20× and 80× magnifications were used to locate a "sparse" region of the sample (see Fig. 2.2). A sparse region was required for optical imaging as regions that contain overly packed erythrocytes are difficult to image. Additionally, an overabundance of cells in a small region cause them to deform from their natural biconcave shape.

Magnifications of 1000× to 1500× were employed for the data collection. About 8 data points were collected within each image/location. Switching back to 20× magnification enabled finding another sparse location within the same blood drop to collect more data. This two-locations-per-drop method was used for each blood drop imaged. 2 drops were taken from each blood sample (i.e. each vial of blood). Thus, in total, 4 locations were imaged per blood sample. The 11/5 experiment had 3 blood samples (for a total of 12 images) and the 12/9 experiment had 5 blood samples (for

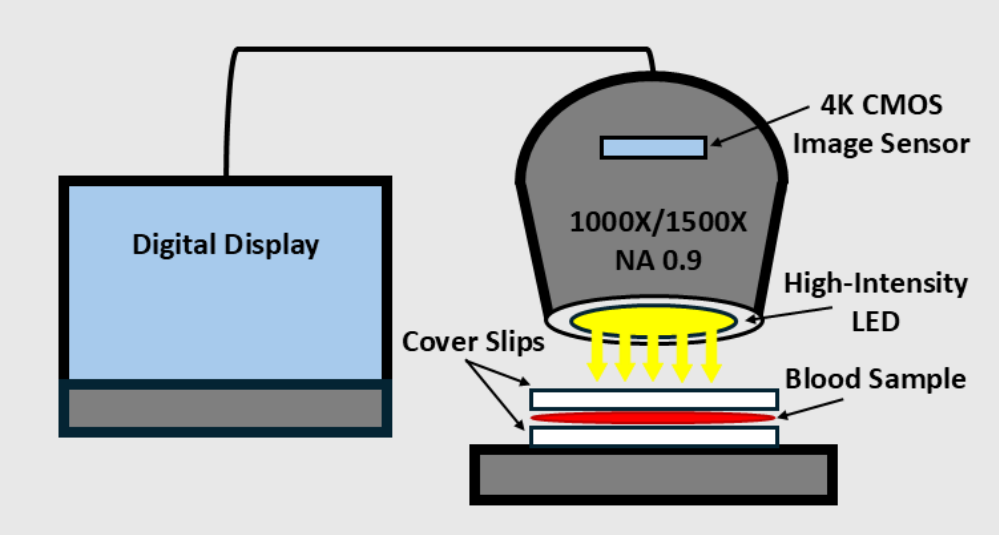

Figure 2.1 Keyence VHX optical microscope schematic. A single drop of blood is placed on a coverslip and a second coverslip is gently placed on top. This creates a small pressure on the blood and maintains a uniform layer of blood between the two coverslips. The full-coaxial setting was selected for illumination. For data collection, 1000× and 1500× magnifications were used. The Keyence is equipped with a 4K complimentary metal-oxide semiconductor (CMOS) image sensor and numerical aperture (NA) of 0.9.

a total of 20 images). This approach yielded approximately 32 data points per vial of blood, thus ensuring good sampling of the large erythrocyte population.

The two-point length measurement tool on the Keyence was used to measure cell diameter. Cells that appeared representative of the average diameter of the cells in the field of view were selected for measurement (i.e. the chosen cell was not overly wide or narrow). This pseudo-random selection of cells minimized outliers while maintaining good representation of the cell population.

For thickness measurements, the Rouleaux formations were analyzed. Formations that were "edge-on" from the viewing perspective (i.e. the smaller dimension of the cells were visible and not the concave faces) were selected for measurement. The same two-point length measurement tool was used to measure the length of the stack by clicking on the outer membrane of the cells on either end of the formation. By dividing this length by the total number of cells in the stack, the average cell thickness was obtained. This constituted a single thickness data point.

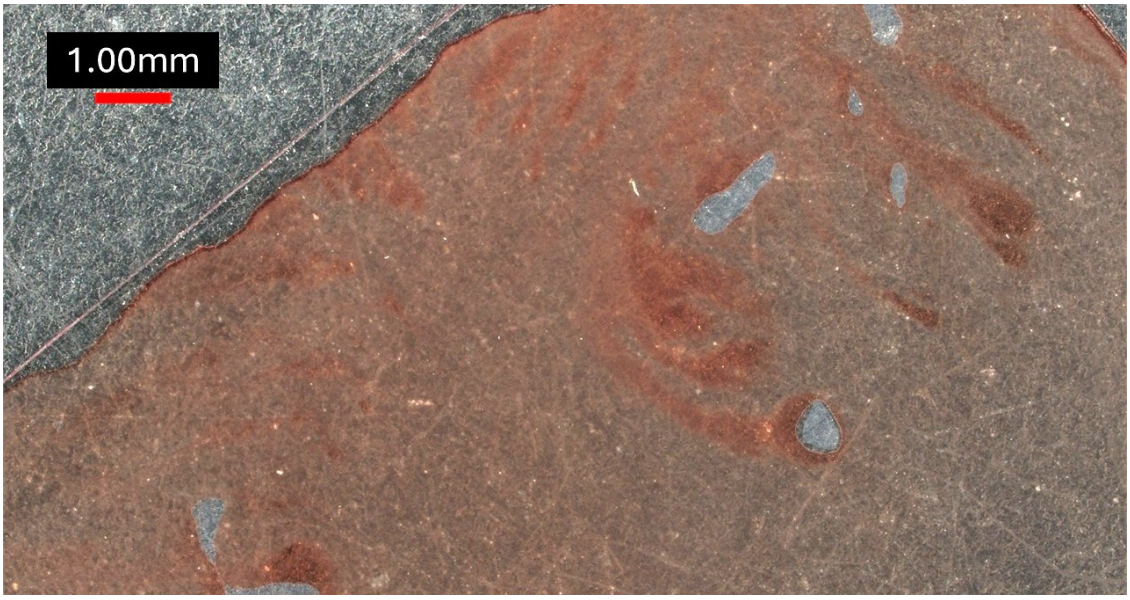

Figure 2.2 View of blood between coverslips at 20× magnification. Note the dense concentration of erythrocytes near the top of the field of view. Contrast to the sparse area in the lower right hand corner.

Note that the 32 thickness data points represent well over 32 cells as each value is an average of 2-10 cells in a Rouleaux formation. Fig. 2.3 is an image of the whole, unaltered blood. Fig. 2.4 shows a blood sample that has had a glucose increase of +1000 mg/dL. Fig. 2.5 shows a blood sample with a glucose increase of +2000 mg/dL.

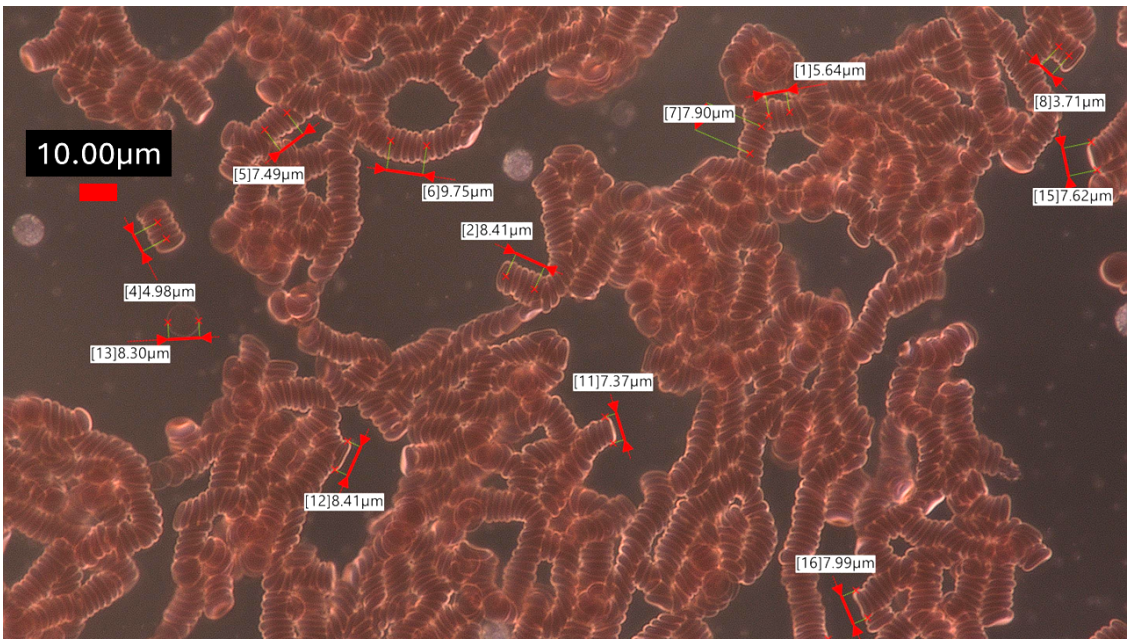

Figure 2.3 Optical micrograph of +0 mg/dL glucose (whole, unaltered blood) sample. Note the significant Rouleaux stacking. The two-point length measurement tool was used to obtain stack height and cell diameter values. Several white blood cells are also seen as gray translucent spheroids.

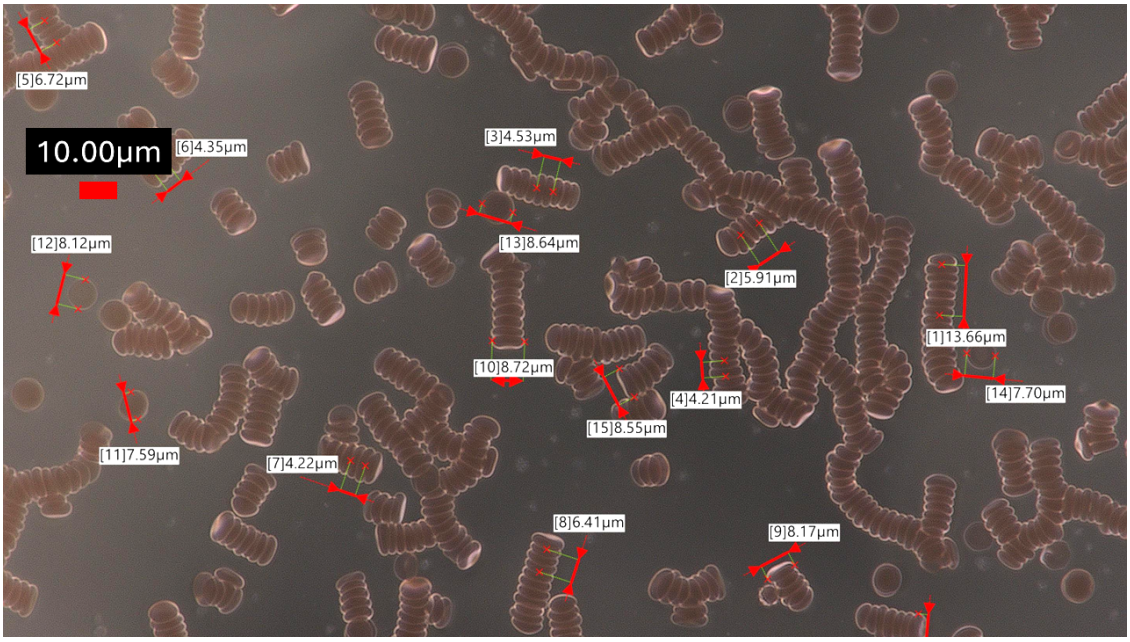

Figure 2.4 Optical micrograph of +1000 mg/dL blood sample. Note the cells are slightly thicker than the unaltered cells (see Fig. 2.3). The two-point length measurement tool was used to obtain stack height and cell diameter values.

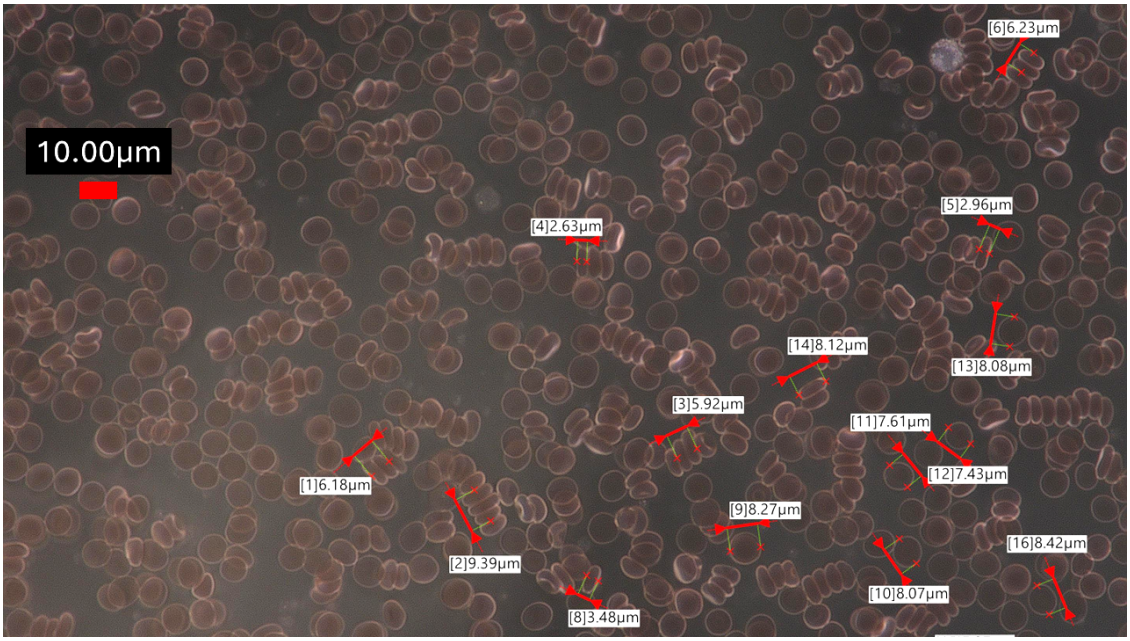

Figure 2.5 Optical micrograph of +2000 mg/dL glucose blood sample. Note the minimal Rouleaux stacking. The two-point length measurement tool was used to obtain stack height and cell diameter values.

Chapter 3

Results

All data points (thickness and diameter) for each sample were averaged and standard deviations were calculated. Diameter values are tabulated in Table 3.1. Thickness values are tabulated in Table 3.2. These data are also plotted in Fig. 3.1 and Fig. 3.2 with standard deviations represented as error bars. Note the missing values are from the 11/5 experiment which did not include glucose increases of +500 mg/dL and +1500 mg/dL.

Due to the minimal change in average cell diameter (as discussed in Section 4.1), it cannot be confidently concluded that erythrocyte diameter is affected following an isosmotic glucose addition (see Fig. 3.1). Average erythrocyte thickness increased 15% following a glucose concentration increase of only +500 mg/dL. For the +1000 mg/dL and +2000 mg/dL samples, average cell thickness increased 22% and 68% respectively.

The data shown in Fig. 3.2 was analyzed by linear regression. The 11/5 experiment data (Fig. 3.1) had a slope of 0.000534 with units of $\frac{\mu m}{+mg/dL}$. The 12/9 experiment data had a slope of 0.000621 $\frac{\mu m}{+mg/dL}$. Note that the 11/5 experiment only used 3 blood samples whereas the 12/9 experiment used 5. Thus, the ratio of data points from the 11/5 experiment to the 12/9 experiment was 3:5. Therefore, in order to generalize the slope that an increase in glucose concentration has on erythrocyte thickness, a weighted average of these slope values was performed. This gave a slope

of 0.000588$\frac{\mu m}{+mg/dL}$. This slope corresponds to a thickness increase of 0.0588 μm per increase in glucose concentration of +100 mg/dL.

Table 3.1 Average erythrocyte diameter results. Avg = "average", SD = "Standard Deviation", exp. = "experiment". Experiment dates are as indicated. Missing values are from the 11/5 experiment which did not test glucose additions of +500 mg/dL and +1500 mg/dL.

Glucose addition	Avg (11/5 exp.)	SD (11/5 exp.)	Avg (12/9 exp.)	SD (12/9 exp.)
+0 mg/dL	8.21 μm	0.43 μm	8.15 μm	0.37 μm
+500 mg/dL	-	-	8.20 μm	0.49 μm
+1000 mg/dL	8.10 μm	0.53 μm	8.12 μm	0.41 μm
+1500 mg/dL	-	-	8.17 μm	0.38 μm
+2000 mg/dL	7.78 μm	0.55 μm	7.86 μm	0.54 μm

Table 3.2 Average erythrocyte thickness results. Avg = "average", SD = "Standard Deviation", exp. = "experiment". Experiment dates are as indicated. Missing values are from the 11/5 experiment which did not test glucose additions of +500 mg/dL and +1500 mg/dL.

Glucose addition	Avg (11/5 exp.)	SD (11/5 exp.)	Avg (12/9 exp.)	SD (12/9 exp.)
+0 mg/dL	1.95 μm	0.16 μm	1.85 μm	0.11 μm
+500 mg/dL	-	-	2.12 μm	0.36 μm
+1000 mg/dL	2.44 μm	0.24 μm	2.27 μm	0.15 μm
+1500 mg/dL	-	-	2.69 μm	0.16 μm
+2000 mg/dL	3.02 μm	0.32 μm	3.12 μm	0.21 μm

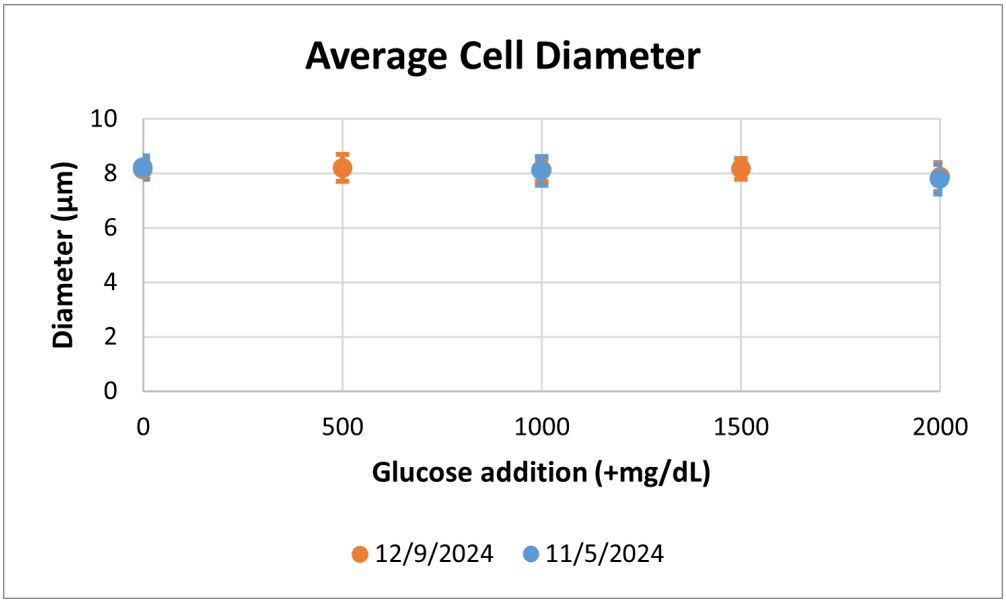

Figure 3.1 Average cell diameter by sample. Error bars represent standard deviations. Due to the significant overlap of error bars and the minimal shift in average value, it cannot be confidently concluded that cell diameter was affected.

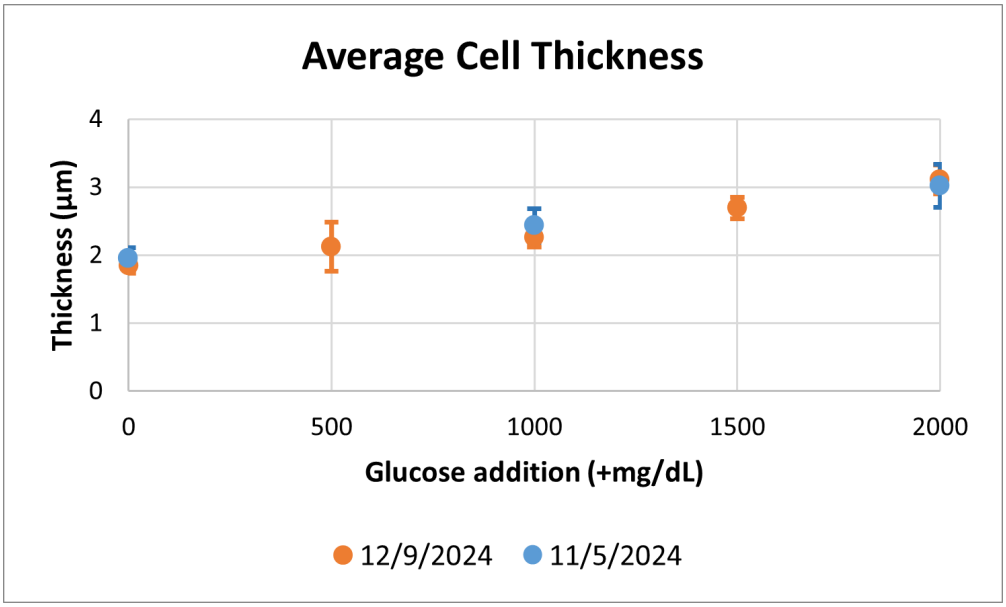

Figure 3.2 Average cell thickness by sample. Error bars represent standard deviations. A clear trend is seen of an increase in average cell thickness following a glucose addition.

Chapter 4

Discussion

In order to connect glucose concentration effects to optical properties of whole blood, erythrocyte morphology is under investigation. Section 3 reports the effect of glucose additions on erythrocyte diameter and thickness. The erythrocyte dimensions reported in Section 3 show that the morphology of the erythrocytes with no glucose added (i.e. whole, unaltered blood) have similar dimensions to those found *in vivo* (which generally have a diameter of 7.5 to 8.7 μm and a thickness of 1.7 to 2.2 μm [17]).

4.1 Cellular Response

As seen in Fig. 3.1, average erythrocyte diameter had little to no change upon addition of glucose. While diameter seemed to drop slightly following the glucose addition of +2000 mg/dL, the overlap of error bars renders any conclusive statement about cell diameter impossible. This is unsurprising as cells tend to maintain an approximately constant surface area (even when swelling or shrinking) due to the strong yet flexible cell membrane.

Erythrocyte thickness, on the other hand, was significantly altered by the increase of glucose concentration. While it is possible the effect of elevated glucose concentration on erythrocyte

thickness may be nonlinear, the effect over the studied range is very nearly linear. Furthermore, within physiologically relevant glucose ranges, the effect is even more likely to be linear. As discussed in Section 1, the use of isosmotic glucose additions ensures any change in morphology is a result of the elevated glucose concentration, not any slight difference in tonicity between the whole blood and the glucose addition.

The optical micrographs seen in Figs. 2.3-2.5 show a decrease in the prevalence of Rouleaux formations. Many more independent cells are seen in higher glucose concentration samples and the average number of cells found in a formation is markedly lower. This is likely due to the substantial change in cell morphology at high glucose concentrations, which may inhibit the cells' ability to aggregate. It should be noted, however, that Rouleaux formations are rarely formed *in vivo*. Thus, these formations were a useful tool in measuring average cell thickness, but their effect in light scattering is not relevant to the present study.

4.2 Morphology Effect on Light Scattering

It was observed by Harkness et al. that increased glucose concentration resulted in reduced scattering [1]. The present work shows that increasing glucose concentration also increases cell thickness. It is possible that the change in erythrocyte morphology in response to a glucose addition is the cause of the decrease in scattering of the blood.

Even though both responses are seen following the same cause (i.e. a glucose addition), a precise mechanism is required before a strong claim can be made connecting these phenomena. Although the size and shape of a scatterer is known to have an effect on the resulting scatter pattern (i.e. the scattering coefficient in the case of blood), more work is required to establish such a cause-and-effect relationship for the optics of blood.

It is well understood that the size and shape of a scattering body will affect the resulting scatter pattern. Think, for example, of classical optics. Simple lenses of varying thicknesses will have different focal points. These lenses bend light due to the difference of refractive index between the air and the glass. Likewise, the difference of index of refraction of erythrocyte and the surrounding plasma dominates the light scattering off of the cells.

However, classical optics is a poor model for light scattering by erythrocytes. Scattering by bodies that have physical dimensions that are comparable to the wavelength of scattered light is more accurately modeled by Mie scattering theory. Unfortunately, the Mie scattering solution can only be solved analytically in the case of a perfect sphere or infinitely long cylinder. Numerical approaches will thus be necessary to model erythrocyte-shaped scattering bodies.

Additionally, the many-body effects on scattering can only be accounted for using computational modeling. While simple assumptions to the Mie theory may yield an approximate scatter pattern from a single cell, blood samples contain billions of cells and therefore require computational approaches.

Computational modeling will need to answer two related but distinct questions. First, how does the morphology of a single cell (or cluster of cells) affect the scatter pattern? Secondly, how does the distribution of morphologies within a bulk blood sample affect overall scattering from the fluid? Each question must be answered for varying cell morphologies arising from glucose concentration alterations. This modeling is required to determine whether the observed morphological changes are sufficient to explain the scattering changes observed by Harkness et al. [1].

4.3 An Alternate Mechanism

While this study has revealed a detectable change in erythrocyte morphology in response to a glucose concentration, there are other possible explanations to account for the change in scattering

of whole blood following similar glucose additions. Refractive index of the plasma may be affected by an increase in glucose concentration. This would affect the difference between the indices of refraction of the plasma and the erythrocytes (which have a mostly constant refractive index). This may also affect the scattering from a single cell.

Some work [18, 19] has even proposed plasma refractometry as a method for invasive glucose measurement. This approach would rely entirely on the effect of glucose on plasma refractive index. However, this relationship would need further study before a strong correlation between light scattering and plasma refractive index could be claimed.

Chapter 5

Conclusion

Understanding the relationship between glucose concentration and the optical properties of whole blood could be crucial for future technologies, and may guide future glucose detection techniques. In this work, the quantified morphology effects of isosmotic glucose additions to whole human blood is presented. Following a glucose addition of +500 mg/dL, erythrocyte thickness increased 15%. This change corresponds to an average cell thickness increase of +0.059 μm per glucose increase of +100 mg/dL. This relationship lays the groundwork for exploration into a more precise mechanistic explanation for the changes in optical properties observed following a glucose increase *in vitro*.

Further work is needed to elucidate a more precise relationship between glucose and the scattering coefficient. Optical modeling may clarify the relationship between erythrocyte morphology and scattering. Given that the principal scattering bodies are similar in size to the wavelength of scattered light, Mie scattering theory must be investigated.

Appendix A

Erythrocyte Images

This chapter contains one image from each blood sample in the experiments described in Chapter 2. Note that the experiment on 12/9/24 used 5 blood samples (+0 mg/dL, +500 mg/dL, +1000 mg/dL, +1500 mg/dL, and +2000 mg/dL), while the experiment on 11/5/24 used only 3 blood samples (+0 mg/dL, +1000 mg/dL, and +2000 mg/dL). The images in this section represent examples from each blood sample, but not all images used for data are shown.

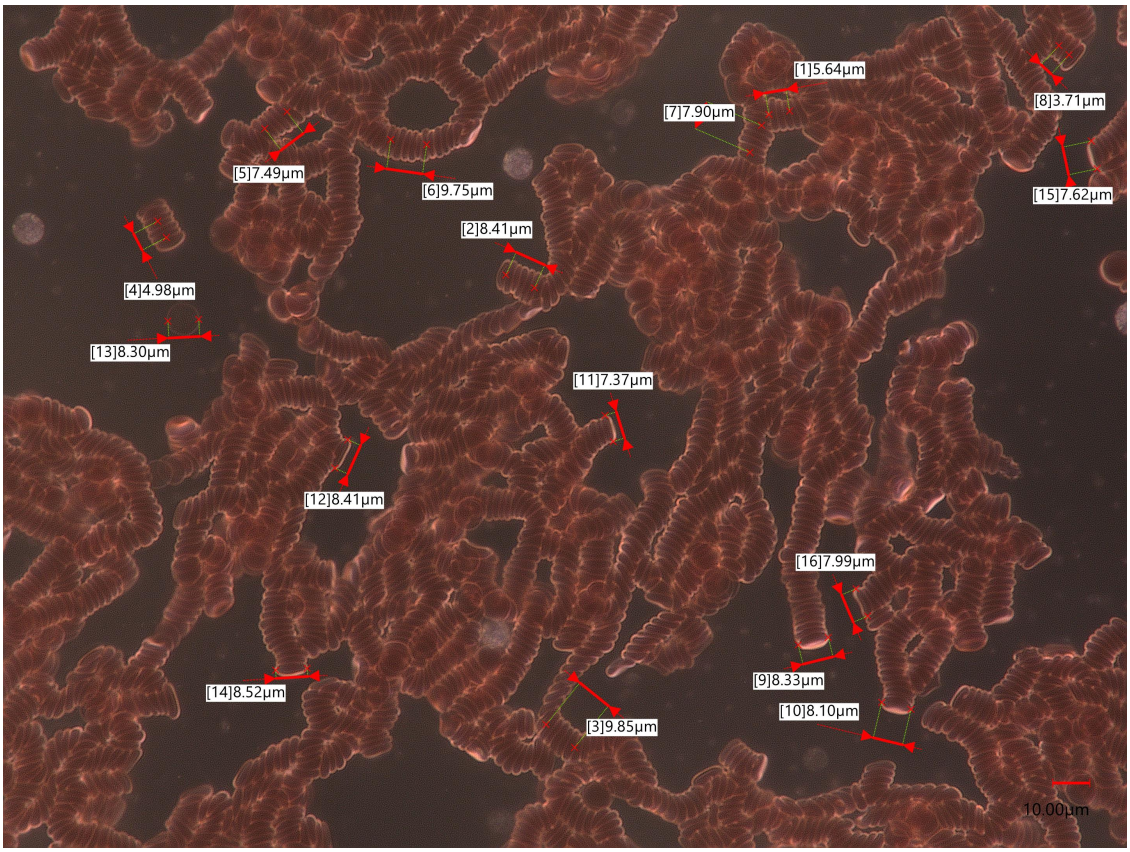

Figure A.1 Whole blood sample from 12/9 experiment.

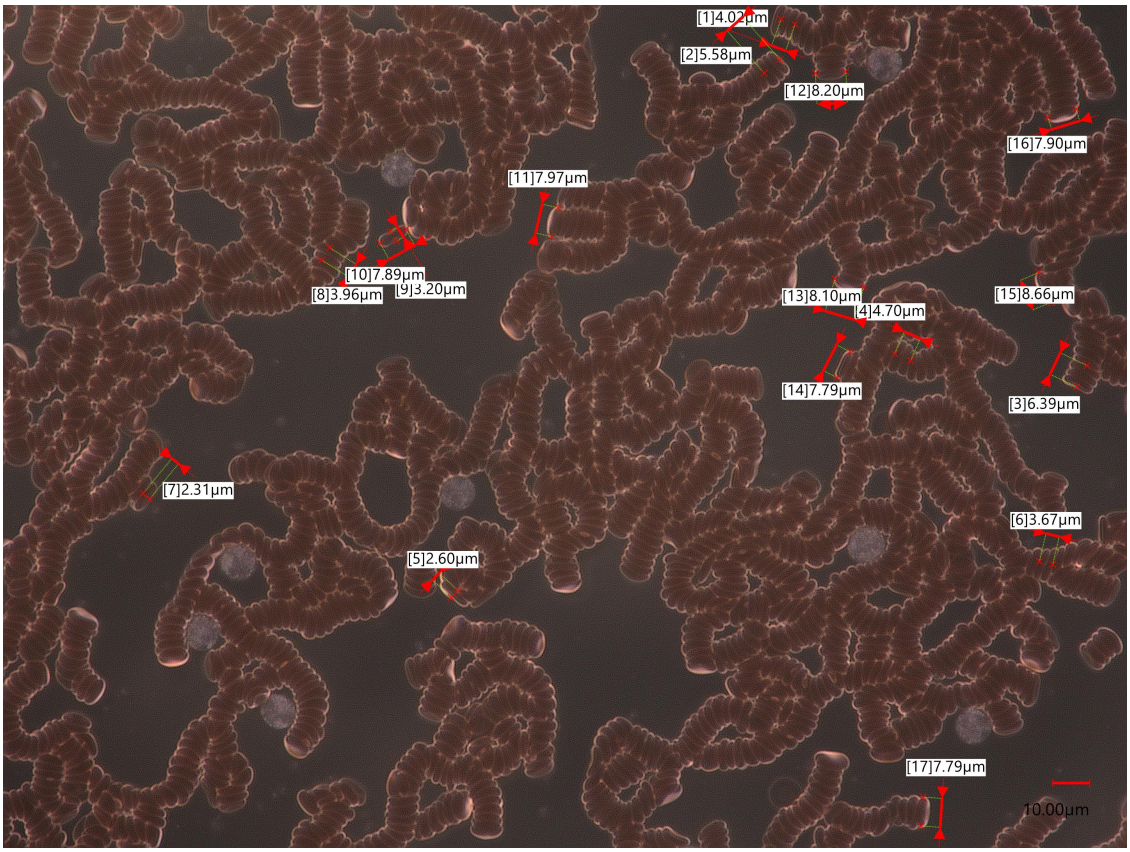

Figure A.2 +500 mg/dL sample from 12/9 experiment.

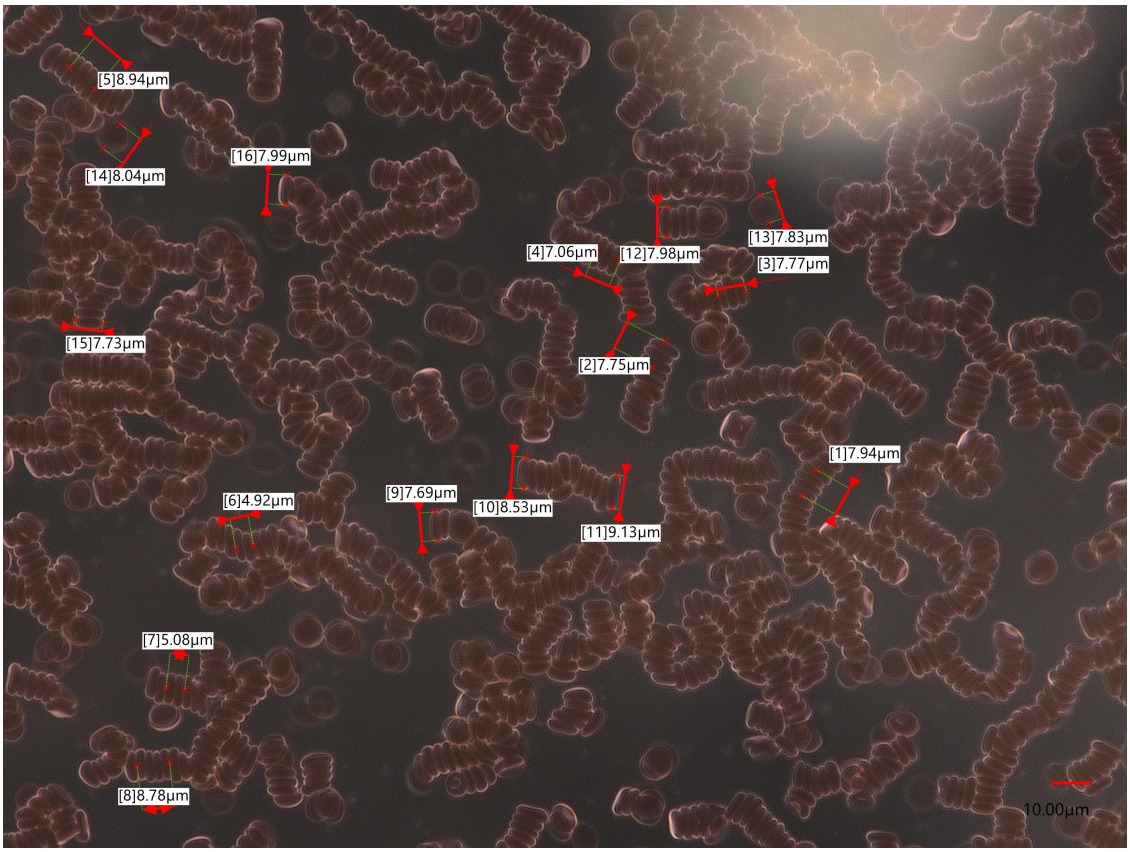

Figure A.3 +1000 mg/dL sample from 12/9 experiment.

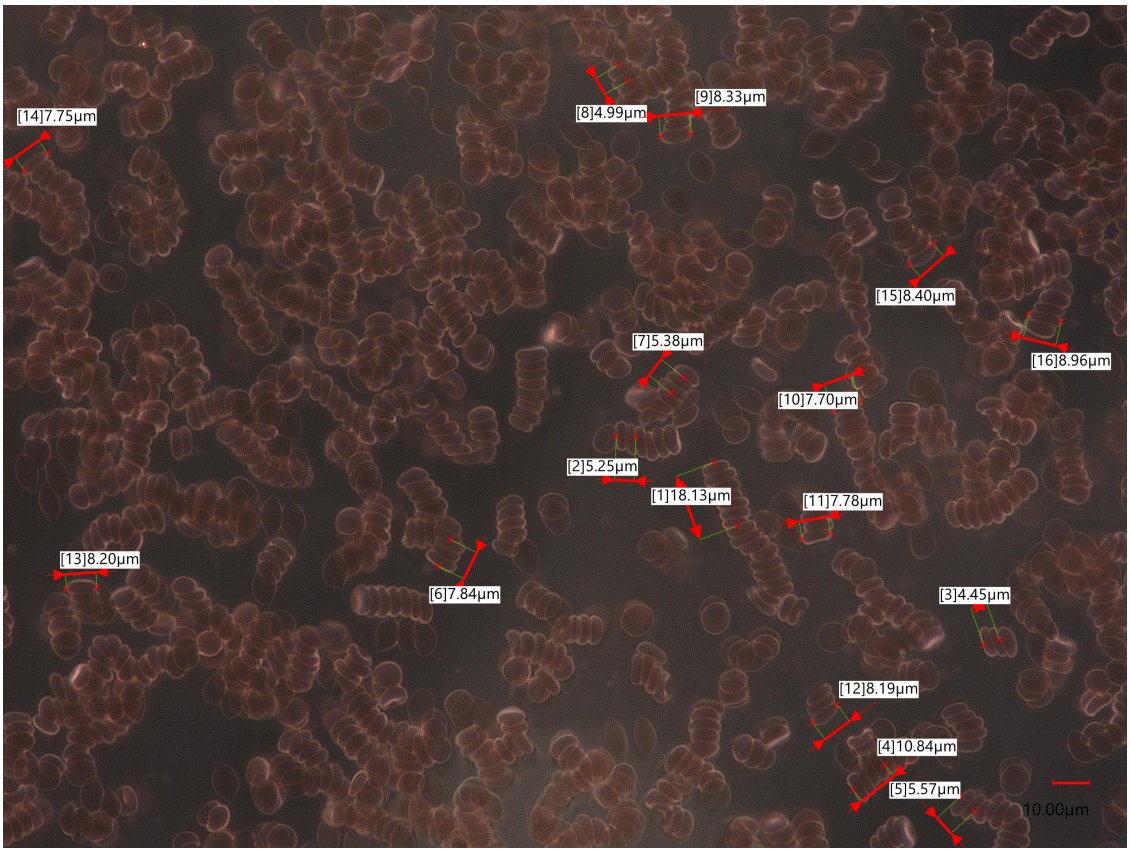

Figure A.4 +1500 mg/dL sample from 12/9 experiment.

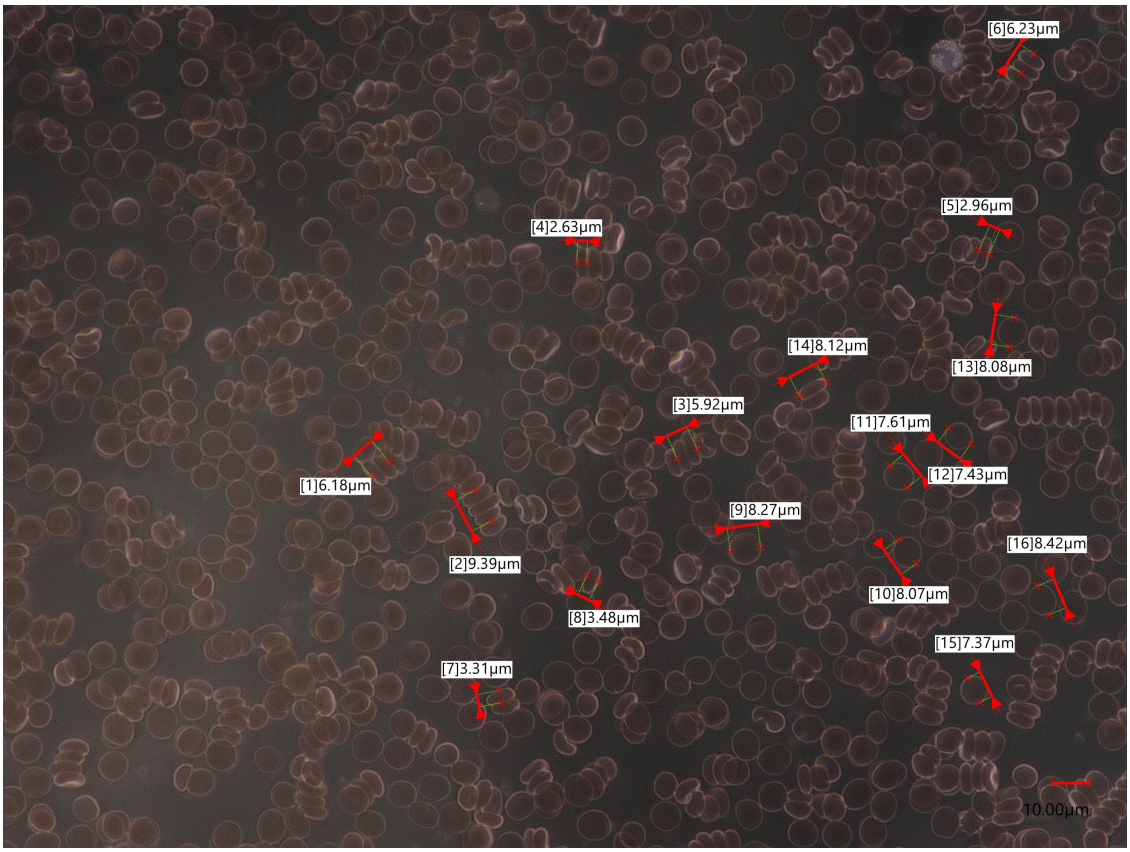

Figure A.5 +2000 mg/dL sample from 12/9 experiment.

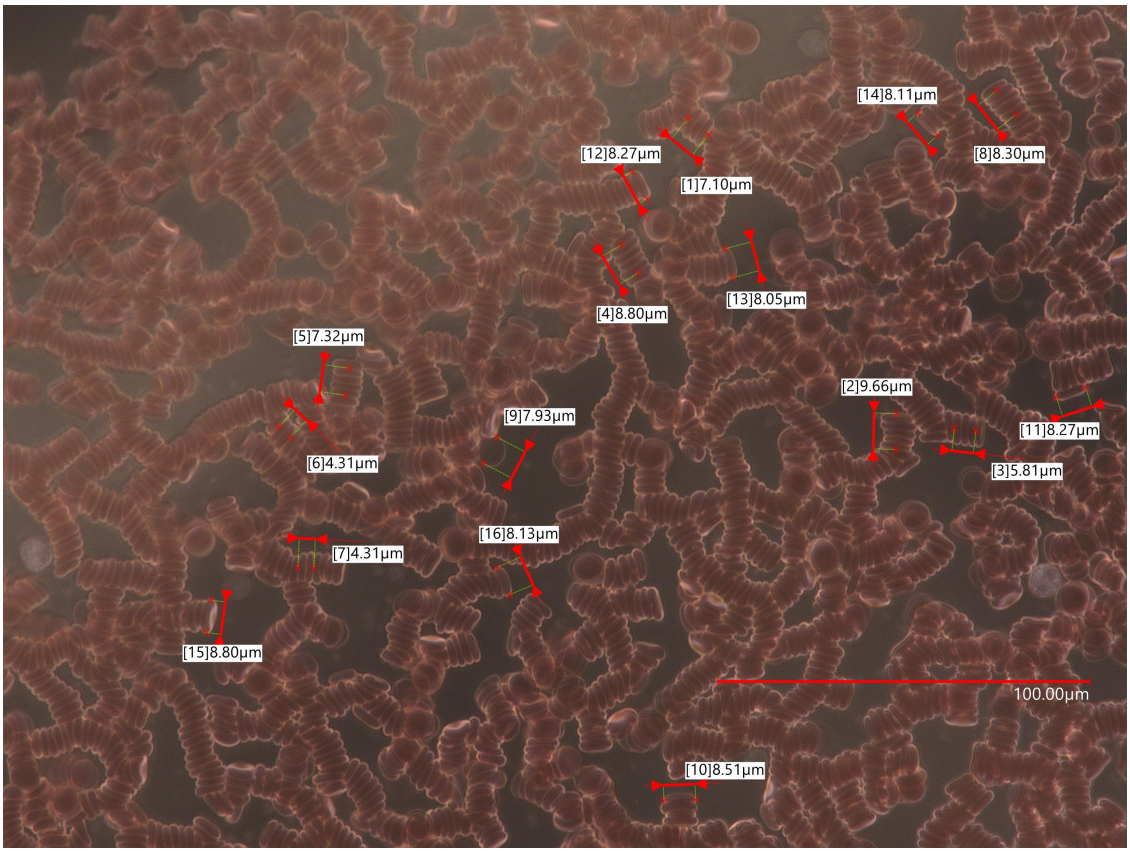

Figure A.6 Whole blood sample from 11/5 experiment.

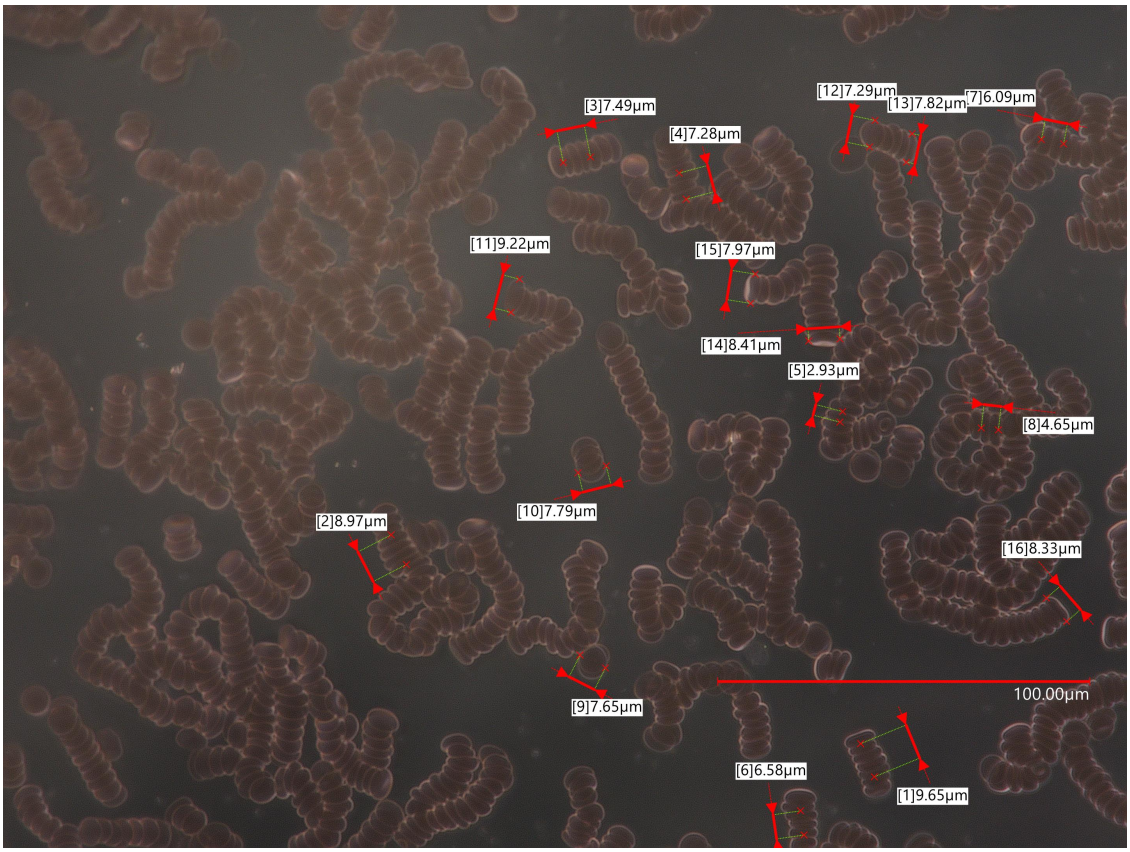

Figure A.7 +1000 mg/dL sample from 11/5 experiment

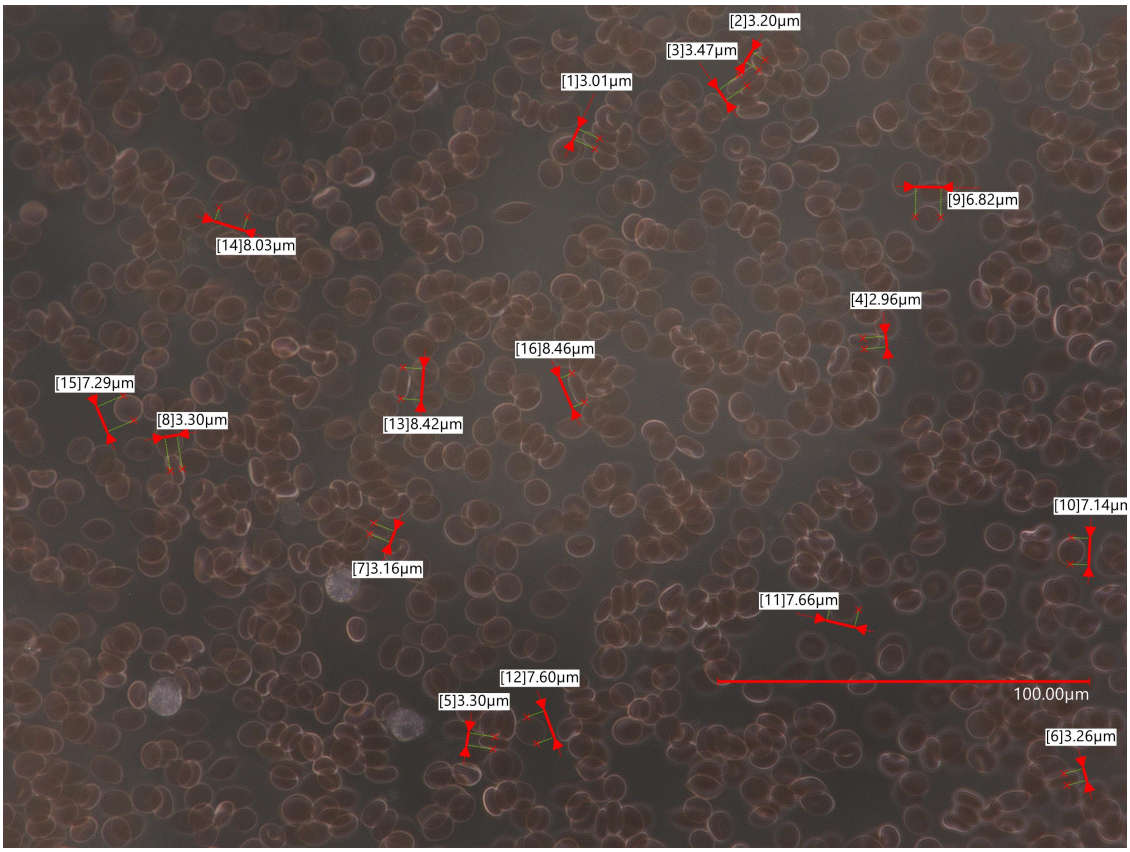

Figure A.8 +2000 mg/dL sample from 11/5 experiment

Bibliography

[1] J. Harkness, "In Vitro Observation of Optical Changes in Whole Blood Due to Injection of Glucose Solution," Masters Thesis, Brigham Young University (2023).

[2] J. Roth, J. Logan, J. Harkness, R. Vanfleet, R. Davis, W. Pitt, and T. Westover, "Optical changes in whole blood versus glucose concentration," In *Biomedical Light Scattering XV*, **13320,** 89–94 (2025).

[3] CDC, "National Diabetes Statistics Report,", 2024.

[4] S. F. Todaro B, Begarani F and L. S, "Is Raman the best strategy towards the development of non-invasive continuous glucose monitoring devices for diabetes management?," Front. Chem. 10 (2022).

[5] FDA, "Do Not Use Smartwatches or Smart Rings to Measure Blood Glucose Levels: FDA Safety Communication,", 2024.

[6] S. A. Pullano, M. Greco, M. G. Bianco, D. Foti, A. Brunetti, and A. S. Fiorillo, "Glucose biosensors in clinical practice: Principles, limits and perspectives of currently used devices," Theranostics **12,** 493 (2022).

[7] A. K. Amerov, J. Chen, G. W. Small, and M. A. Arnold, "Scattering and absorption effects in the determination of glucose in whole blood by near-infrared spectroscopy," Analytical chemistry **77,** 4587–4594 (2005).

[8] P. C. et al., in *Veterinary Medicine (11th ed.)* (2017), Chap. 5 - Disturbances of Free Water, Electrolytes, Acid-Base Balance, and Oncotic Pressure.

[9] R. Zhong, D. Han, X. Wu, H. Wang, W. Li, Z. He, X. Zhang, and J. Liu, "An evaluation of morphological changes and deformability of suspended red blood cells prepared using whole blood with different hemoglobin levels of Tibetans," Transfusion Medicine and Hemotherapy **48,** 210–219 (2021).

[10] J. J. Bishop, P. R. Nance, A. S. Popel, M. Intaglietta, and P. C. Johnson, "Relationship between erythrocyte aggregate size and flow rate in skeletal muscle venules," American Journal of Physiology-Heart and Circulatory Physiology **286,** H113–H120 (2004).

[11] J. Mauer, M. Peltomäki, S. Poblete, G. Gompper, and D. A. Fedosov, "Static and dynamic light scattering by red blood cells: A numerical study," PLoS One **12,** e0176799 (2017).

[12] G. Marcelli, K. H. Parker, and C. P. Winlove, "Thermal fluctuations of red blood cell membrane via a constant-area particle-dynamics model," Biophysical Journal **89,** 2473–2480 (2005).

[13] A. G. Borovoi, E. I. Naats, and U. G. Oppel, "Scattering of light by a red blood cell," Journal of biomedical optics **3,** 364–372 (1998).

[14] G. J. Streekstra, A. G. Hoekstra, E.-J. Nijhof, and R. M. Heethaar, "Light scattering by red blood cells in ektacytometry: Fraunhofer versus anomalous diffraction," Applied Optics **32,** 2266–2272 (1993).

[15] P. Sloot and C. G. Figdor, "Elastic light scattering from nucleated blood cells: rapid numerical analysis," Applied Optics **25,** 3559–3565 (1986).

[16] A. G. Hoekstra, J. A. Aten, and P. Sloot, "Effect of aniosmotic media on the volume of the T-lymphocyte nucleus," Biophysical Journal **59,** 765–774 (1991).

[17] M. Diez-Silva, M. Dao, J. Han, C.-T. Lim, and S. Suresh, "Shape and biomechanical characteristics of human red blood cells in health and disease," MRS bulletin **35,** 382–388 (2010).

[18] K. Zirk and H. Poetzschke, "On the suitability of refractometry for the analysis of glucose in blood-derived fluids," Medical engineering & physics **26,** 473–481 (2004).

[19] K. Zirk and H. Poetzschke, "A refractometry-based glucose analysis of body fluids," Medical engineering & physics **29,** 449–458 (2007).

Index